

## Methane Oxidation over Alumina-Supported Noble Metal Catalysts with and without Cerium Additives

SE H. OH,\* PATRICIA J. MITCHELL,\* AND ROBERT M. SIEWERT†

\*Physical Chemistry Department and †Thermosciences Department, General Motors Research Laboratories, Warren, Michigan 48090

Received March 8, 1991; revised July 3, 1991

Laboratory reactor experiments have been conducted to evaluate alumina-supported noble metal catalysts, both in the presence and absence of cerium additives, for their effectiveness in the catalytic oxidation of methane under conditions likely to be encountered in natural-gas vehicle exhaust. Under oxidizing conditions, all of the catalysts promoted the complete oxidation of methane to CO<sub>2</sub> and H<sub>2</sub>O, with the methane oxidation activity ranking given by Pd > Rh > Pt in the absence of Ce and by Rh > Pd ≈ Pt in the presence of Ce. Under reducing conditions, methane oxidation produced substantial amounts of CO and H<sub>2</sub> as the principal partial oxidation products. In the absence of Ce, the methane oxidation activity decreases in the order Pd > Rh > Pt, with the tendency to form CO decreasing in the order Rh > Pd > Pt. The activity ranking for methane conversion in reducing feedstreams was not affected by the presence of Ce; however, the addition of Ce to the Pt/Al<sub>2</sub>O<sub>3</sub> and Pd/Al<sub>2</sub>O<sub>3</sub> catalysts almost completely suppressed the formation of the partial oxidation product CO. At a fixed temperature of ~550°C, the methane conversion over each of the noble metal catalysts goes through a maximum as the feedstream concentration of O<sub>2</sub> is varied. The data suggest that O<sub>2</sub> inhibits the CH<sub>4</sub> oxidation under oxidizing conditions by excluding the more weakly adsorbed species, CH<sub>4</sub>, from the active sites. Also, methane oxidation experiments in the presence of CO in the feed showed that the methane conversion characteristics of the noble metal catalysts are little affected by the CO. © 1991 Academic Press, Inc.

### INTRODUCTION

In recent years natural gas has received increased attention as an alternative fuel for motor vehicles because of its potential technical, economic, and environmental advantages. Natural gas, which consists primarily of methane, has excellent knock resistance and ignition capability over a wide range of air-fuel ratios (1). These properties permit natural-gas engines to operate at high compression ratios and with very fuel-lean mixtures, resulting in substantially higher fuel efficiencies than are possible with gasoline engines. Also, natural gas is less expensive than gasoline on an energy basis and is expected to be available well into the next century (2). Environmental benefits of natural gas include extremely low photochemical reactivity (3), reduced cold-start CO emissions (1), and zero evaporative emis-

sions. Furthermore, the low carbon content of methane would lead to reduced CO<sub>2</sub> emissions (the most common "greenhouse" gas) from natural-gas vehicles. However, methane itself is a much more powerful greenhouse gas than CO<sub>2</sub> (4, 5) and thus, although not currently regulated, exhaust emissions of unburned methane from natural-gas vehicles are anticipated to be of particular concern in the future.

Vehicle emission tests conducted at General Motors Research Laboratories with two different gasoline engines converted to operate on natural gas (6) showed that poor methane conversion (<15% during FTP) occurs over commercial three-way catalysts currently used for gasoline-vehicle exhaust emission control. These dual-fuel vehicles were designed to operate open-loop (lean) when running on compressed natural gas. This observation of low methane conversion

in the lean natural-gas engine exhaust is not surprising in view of previous reports in the literature (Ref. (7) and references therein), which generally show that methane is the most difficult hydrocarbon to oxidize catalytically. The results of these vehicle emission tests also indicate that the optimal catalyst formulation for natural-gas vehicles may differ from that for gasoline vehicles.

This laboratory reactor study was initiated to investigate the possibility of controlling methane emissions by catalytic oxidation of unburned methane present in natural-gas engine exhaust. Most of the previous laboratory studies on the catalytic oxidation of methane [e.g., Refs. (7-11)] focused on experimental conditions where there is an excess of oxygen over methane (i.e.,  $O_2/CH_4 > 2$ ). Because of the wide ignition range of natural gas, however, actual natural gas engines can potentially be operated under a variety of air-fuel ratio conditions. The currently favored operating strategies for natural-gas engines include fuel-lean and stoichiometric combustion (1). Since catalytic activity is often a sensitive function of the stoichiometry of the reaction environment (12), it is entirely possible that methane conversion efficiency in natural-gas engine exhaust may vary substantially with the air-fuel ratio. With this possibility in mind, we conducted laboratory methane oxidation experiments with single-component noble metal catalysts over wide ranges of temperatures and feedstream stoichiometries. The results of such laboratory experiments are of practical interest because (1) methane is the principal hydrocarbon species in natural-gas engine exhaust, (2) its oxidation characteristics have not been examined under conditions likely to be encountered in natural-gas vehicle exhaust, and (3) noble metals are ranked among the most active catalysts for methane oxidation (7, 8).

#### EXPERIMENTAL

##### *Catalysts*

Two sets of Pt, Pd, and Rh catalysts were used in this study: one supported on spheres

of  $\gamma$ -alumina (3 mm diameter, 96  $m^2/g$  BET area) and the other on spheres of Ce-modified alumina (6 wt% Ce uniformly distributed, 3.4 mm diameter, 125  $m^2/g$  BET area). All of the catalysts were prepared by incipient wetness impregnation with aqueous solutions of the metal salts. The metal loadings, metal salts used in the preparation, and CO/metal and H/metal ratios determined from static chemisorption measurements are listed in Table 1. After impregnation, the catalysts were dried in air overnight at room temperature and then calcined in flowing air at 500°C for 4 h. Such procedures resulted in the deposition of the noble metals near the periphery of the catalyst beads. The observation of a CO/Rh atomic ratio in excess of unity for Rh/ $Al_2O_3$  indicates that at least part of the Rh exists as isolated atoms or ions, forming a dicarbonyl species during CO chemisorption (13, 14).

##### *Reactor System and Analytical Methods*

The integral flow reactor system used in this study was similar to that employed in a previous study (15). The reactor was a 2.5-cm-o.d. stainless-steel tube housed in an electric furnace. The feed gases were passed downward through layers of silicon carbide particles and the catalyst pellets. The silicon carbide layer located upstream of the catalyst bed serves as an inert heat transfer medium and also helps establish fully developed flow in the reactive section. Temperatures were measured with a chromel-alumel thermocouple positioned along the reactor centerline with its tip located a few millimeters below the top of the catalyst bed. All the experiments reported here were performed using 15  $cm^3$  of catalyst and a total feedstream flow rate of 13 liter/min (STP), yielding a space velocity of 52,000  $h^{-1}$ . The feedstream contained 0.2 vol%  $CH_4$ , 0.1 vol% CO if present, and variable levels of  $O_2$  in a He background.

The gas stream entering and leaving the reactor was analyzed using a Varian 6000 gas chromatograph equipped with a thermal conductivity detector. A single column

TABLE 1  
Catalyst Properties

Catalyst	Metal loading (wt%)	Noble metal precursor	Chemisorption	
			CO/M	H/M
Pt/Al <sub>2</sub> O <sub>3</sub>	0.20 Pt	H <sub>2</sub> PtCl <sub>6</sub>	0.60	0.70
Pd/Al <sub>2</sub> O <sub>3</sub>	0.16 Pd	PdCl <sub>2</sub>	0.21	0.32
Rh/Al <sub>2</sub> O <sub>3</sub>	0.14 Rh	RhCl <sub>3</sub>	1.25	0.42
Pt/Ce/Al <sub>2</sub> O <sub>3</sub>	0.19 Pt, 6 Ce	H <sub>2</sub> PtCl <sub>6</sub>	0.74	0.81
Pd/Ce/Al <sub>2</sub> O <sub>3</sub>	0.14 Pd, 6 Ce	PdCl <sub>2</sub>	0.33	0.22
Rh/Ce/Al <sub>2</sub> O <sub>3</sub>	0.13 Rh, 6 Ce	RhCl <sub>3</sub>	0.95	0.58

(0.32-cm diameter by 1.5-m length) containing molecular sieve 5A was employed, and the chromatographic separations were carried out isothermally at 60°C in a He carrier gas. Individual species in the reaction mixture were identified and quantified by comparing their elution times and integrated areas with those of commercially supplied calibration gases.

The methane oxidation activity of the catalysts was characterized in two ways: (1) temperature run-up experiments with fixed feed composition and (2) variable composition experiments at a fixed temperature. Assessing catalyst behavior using an integral reactor is fraught with uncertainties, especially when highly exothermic reactions such as methane oxidation are occurring in the system. Temperature and concentration gradients, both in the axial and radial directions, can be quite large at high reactant conversions. (The adiabatic temperature rises are 62 and 53°C with and without CO in the feed, respectively.) Furthermore, temperatures and concentrations within the bed are dependent upon the catalytic activity of the sample being tested, and thus it is difficult to control or even characterize the reaction environment of the catalyst very precisely. However, since our primary interest here is in evaluating catalysts for potential automotive application, we chose to measure catalyst performance under carefully controlled *inlet* conditions to the catalyst bed. The reactor temperature was con-

trolled by a thermocouple placed at the outside surface of the reactor tube. However, temperature values quoted in this study (referred to as catalyst temperature) are those actually measured just below the top of the catalyst bed.

## RESULTS

### *Oxidation Activity of Noble Metal Catalysts in CH<sub>4</sub>-CO-O<sub>2</sub> Mixtures*

Although our principal focus is on the catalytic oxidation of methane, we first conducted laboratory reactor evaluations of the three noble metals Pt, Pd, and Rh in feedstreams that contained CO in addition to methane and O<sub>2</sub>. Carbon monoxide, which is present in natural-gas vehicle exhaust in significant quantities (6), has been shown to significantly affect the oxidation activity of noble metal catalysts for some hydrocarbons (16-18). Furthermore, the presence of CO in the feedstream allows one to examine the conversion efficiencies of both methane and CO simultaneously.

Figure 1 shows the steady-state conversions of CH<sub>4</sub> and CO as a function of temperature for the Pt/Al<sub>2</sub>O<sub>3</sub>, Pd/Al<sub>2</sub>O<sub>3</sub>, and Rh/Al<sub>2</sub>O<sub>3</sub> catalysts. The experiments were conducted in an oxidizing feedstream containing 0.2 vol% CH<sub>4</sub>, 0.1 vol% CO, and 1 vol% O<sub>2</sub>. The CO conversion over the Pt/Al<sub>2</sub>O<sub>3</sub> and Pd/Al<sub>2</sub>O<sub>3</sub> catalysts is near 100% at temperatures as low as ~200°C; however, the Rh/Al<sub>2</sub>O<sub>3</sub> catalyst was observed to be much less active for CO oxidation in this

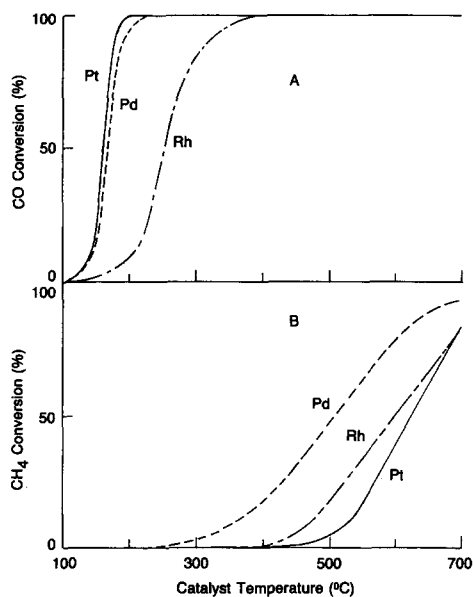


FIG. 1. Conversions of CO (A) and  $\text{CH}_4$  (B) over the alumina-supported noble metal catalysts as a function of temperature in an oxidizing feedstream containing 0.2 vol%  $\text{CH}_4$ , 0.1 vol% CO, and 1 vol%  $\text{O}_2$ .

oxidizing environment, requiring  $\sim 350^\circ\text{C}$  for complete CO conversion.

In agreement with earlier literature reports of extremely low methane oxidation rates (10, 11, 19), high temperatures in excess of  $500^\circ\text{C}$  are required for 50% conversion of the methane over the noble metals in the oxidizing feedstream employed in Fig. 1. The low reactivity of  $\text{CH}_4$  toward  $\text{O}_2$  is also reflected in the absence of catalyst lightoff during the methane oxidation. The methane oxidation activity in the presence of excess  $\text{O}_2$  decreases in the order  $\text{Pd}/\text{Al}_2\text{O}_3 > \text{Rh}/\text{Al}_2\text{O}_3 > \text{Pt}/\text{Al}_2\text{O}_3$ , and this activity ranking is consistent with the observations of Firth and Holland (9) and of Yu Yao (10). In the oxidizing feedstream of Fig. 1, carbon dioxide was the only carbon-containing reaction product detected at temperatures above  $200^\circ\text{C}$  (where the CO in the feed was completely converted), indicating the complete oxidation of the methane in the feed. Complete oxidation of methane was also ob-

served in CO-free oxidizing feeds, as discussed later in this paper.

Since the exhaust composition of actual natural-gas vehicles can fluctuate to the fuel-rich as well as the fuel-lean side of the stoichiometric point, it is of practical interest to examine the performance of the noble metal catalysts under net-reducing conditions. Figure 2 shows steady-state  $\text{CH}_4$  and CO conversions as a function of temperature in a reducing feedstream containing 0.2 vol%  $\text{CH}_4$ , 0.1 vol% CO, and 0.33 vol%  $\text{O}_2$ . All three noble metals exhibit very similar low-temperature CO oxidation activity, reaching nearly 100% CO conversion at temperatures as low as  $200^\circ\text{C}$ . However, the CO conversion efficiencies over the noble metal catalysts begin to fall below 100% near  $450^\circ\text{C}$  and then continue to decline with a further increase in temperature. For each of the noble metal catalysts, the temperature required for the onset of the  $\text{CH}_4$  oxidation in the reducing feedstream of Fig. 2 is similar

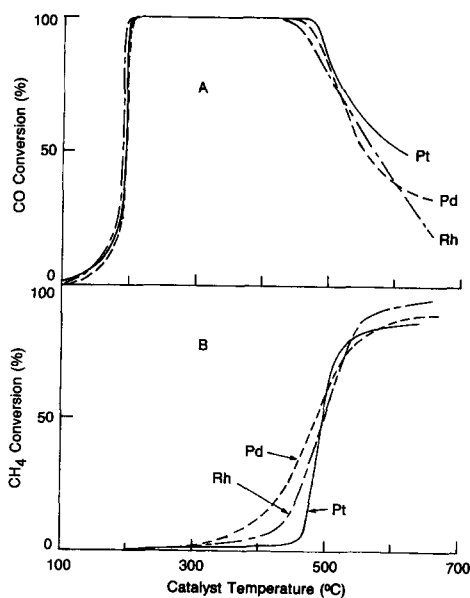


FIG. 2. Conversions of CO (A) and  $\text{CH}_4$  (B) over the alumina-supported noble metal catalysts as a function of temperature in a reducing feedstream containing 0.2 vol%  $\text{CH}_4$ , 0.1 vol% CO, and 0.33 vol%  $\text{O}_2$ .

to that observed in Fig. 1 for the oxidizing feedstream. Note, however, that once the reaction began, the  $\text{CH}_4$  conversion increased much more sharply with temperature (leveling off between 80 and 95% for  $T > 550^\circ\text{C}$ ) in the reducing feedstream than it does in the oxidizing feedstream. The observation that the decrease in CO conversion is generally accompanied by an increase in  $\text{CH}_4$  conversion in Fig. 2 strongly suggests that the loss in CO conversion efficiency at elevated temperatures is due primarily to partial oxidation of methane to CO under the oxygen-deficient conditions. In fact, our experiments with  $\text{CH}_4\text{-O}_2$  mixtures (i.e., no CO in the feed) under reducing conditions confirmed the formation of CO as the principal carbon-containing partial oxidation product of methane oxidation. This aspect is discussed later in the paper.

Comparison of Figs. 1B and 2B shows that at temperatures above  $500^\circ\text{C}$  the  $\text{CH}_4$  conversion over each of the noble metal catalysts is higher in the reducing environment than it is in the oxidizing environment. This suggests the possibility that the  $\text{CH}_4$  conversion may be sensitive to the stoichiometry of the gas-phase environment and thus there may exist an optimum feedstream stoichiometry at which a maximum  $\text{CH}_4$  conversion occurs. To explore this possibility, we measured steady-state  $\text{CH}_4$  and CO conversions at a catalyst temperature of  $\sim 550^\circ\text{C}$  using feedstreams containing 0.2 vol%  $\text{CH}_4$ , 0.1 vol% CO, and variable levels of  $\text{O}_2$ . A wide range of feedstream stoichiometries was covered by increasing the  $\text{O}_2$  concentration step-by-step while holding the temperature and total flow rate constant. The results of such experiments are shown in Fig. 3, where the  $\text{CH}_4$  and CO conversions are plotted against the  $\text{O}_2$  concentration in the feed. It can be seen in Fig. 3B that for each of the noble metal catalysts, the  $\text{CH}_4$  conversion goes through a maximum at an  $\text{O}_2$  concentration somewhat less than its stoichiometric value of 0.45 vol% (i.e., in a net-reducing feed) and then declines sharply as the  $\text{O}_2$

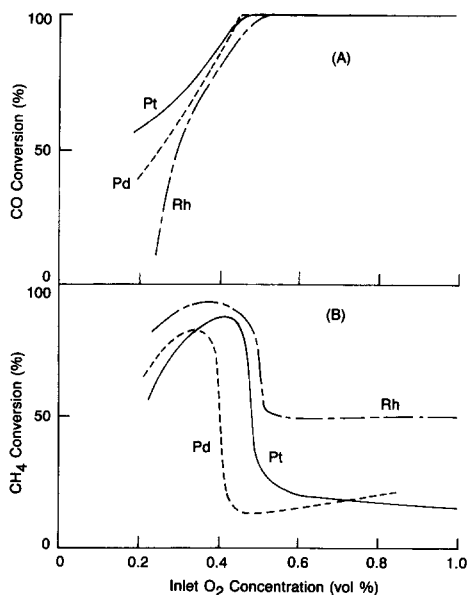


FIG. 3. Conversions of CO (A) and  $\text{CH}_4$  (B) over the alumina-supported noble metal catalysts at a catalyst temperature of  $550^\circ\text{C}$  in feedstreams containing 0.2 vol%  $\text{CH}_4$ , 0.1 vol% CO, and variable levels of  $\text{O}_2$ .

concentration is increased further. The optimum inlet oxygen concentration for Pt/ $\text{Al}_2\text{O}_3$  and Rh/ $\text{Al}_2\text{O}_3$  lies between 0.40 and 0.42 vol%  $\text{O}_2$ ; however, a maximum  $\text{CH}_4$  conversion over Pd/ $\text{Al}_2\text{O}_3$  was observed at a lower inlet  $\text{O}_2$  concentration of  $\sim 0.35$  vol%. The CO conversions measured during the same experiments are plotted in Fig. 3A. For all three noble metal catalysts, the CO conversion increases monotonically with increasing  $\text{O}_2$  concentration in the feed, reaching an asymptotic level of 100% at an  $\text{O}_2$  concentration between 0.45 and 0.5 vol%. Under reducing conditions, the CO conversion efficiency decreases in the order Pt/ $\text{Al}_2\text{O}_3 >$  Pd/ $\text{Al}_2\text{O}_3 >$  Rh/ $\text{Al}_2\text{O}_3$ .

#### *Oxidation Activity of Noble Metal Catalysts in $\text{CH}_4\text{-O}_2$ Mixtures*

Additional methane oxidation experiments were carried out over the same alumina-supported noble metal catalysts without CO in the feed. Comparison of the

results of these experiments with those presented in the previous section allows one to examine how the  $\text{CH}_4$  conversion characteristics of the noble metal catalysts are affected by the presence of CO in the feed. Also, experiments under conditions where CO is absent in the reactant gas mixture provide useful insight into the origin of the CO observed during our previous methane oxidation experiments in a reducing environment and the tendencies of the various noble metals to partially oxidize methane to CO.

Temperature run-up experiments conducted in an oxidizing  $\text{CH}_4\text{-O}_2$  feedstream (0.2 vol%  $\text{CH}_4$ , 1 vol%  $\text{O}_2$ , no CO) revealed methane conversion characteristics similar to those depicted in Fig. 1B. Although not shown, the methane oxidation over each of the noble metal catalysts in the absence of CO began at a temperature comparable to that required for the CO-containing oxidizing feed of Fig. 1. As was also observed in Fig. 1B, the onset of the reaction was followed by a gradual increase in methane conversion with temperature (i.e., absence of catalyst lightoff), although the conversion over  $\text{Pd}/\text{Al}_2\text{O}_3$  and  $\text{Rh}/\text{Al}_2\text{O}_3$  was somewhat more sensitive to temperature in the absence of CO than in the presence of CO. Furthermore, in agreement with the results of Fig. 1B, the methane oxidation activity in the CO-free oxidizing feed was found to decrease in the order  $\text{Pd}/\text{Al}_2\text{O}_3 > \text{Rh}/\text{Al}_2\text{O}_3 > \text{Pt}/\text{Al}_2\text{O}_3$ , forming  $\text{CO}_2$  as the only carbon-containing reaction product (i.e., complete oxidation of methane). The observation that the  $\text{CH}_4$  conversion characteristics during a temperature run-up are essentially unaffected by CO in the feed is not surprising in view of the large disparity in their reactivity toward  $\text{O}_2$ . That is, much higher temperatures are required for methane oxidation than for CO oxidation, so that all the CO has been completely reacted by the time the  $\text{CH}_4$  conversion becomes significant (see Fig. 1).

Similarly, the methane conversion vs temperature data over the noble metal cata-

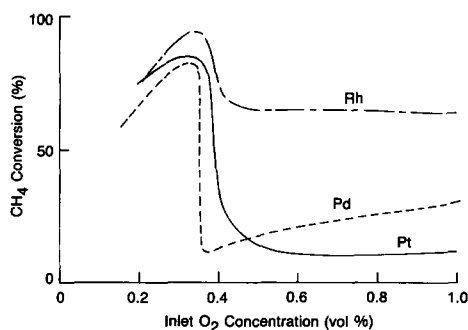


FIG. 4.  $\text{CH}_4$  conversion over the alumina-supported noble metal catalysts at a catalyst temperature of  $550^\circ\text{C}$  in feedstreams containing 0.2 vol%  $\text{CH}_4$  and variable levels of  $\text{O}_2$ .

lysts under reducing conditions were also little affected by the presence of CO in the feed. Temperature run-up experiments with a reducing feedstream containing 0.2 vol%  $\text{CH}_4$ , 0.33 vol%  $\text{O}_2$ , and no CO yielded methane conversion data similar to those shown in Fig. 2B. The similarities in methane oxidation features between the cases with and without CO include (1) the onset of methane oxidation at a comparable temperature for each of the noble metals, (2) the same activity ranking ( $\text{Pd}/\text{Al}_2\text{O}_3 > \text{Rh}/\text{Al}_2\text{O}_3 > \text{Pt}/\text{Al}_2\text{O}_3$ ) for low methane conversions, and (3) similar asymptotic methane conversion levels of  $\sim 90\%$  for temperatures above  $550^\circ\text{C}$ . Again, the insensitivity of  $\text{CH}_4$  conversion to the added CO under reducing conditions can be attributed to complete CO conversion at temperatures where the  $\text{CH}_4$  begins to react (see Fig. 2).

Although added CO does not directly affect  $\text{CH}_4$  conversion characteristics on either side of the stoichiometric point, it consumes oxygen in the feed and consequently changes the value of the critical inlet  $\text{O}_2$  concentration at which an abrupt decline in methane conversion occurs. This aspect becomes apparent when the methane conversion vs  $\text{O}_2$  concentration data of Fig. 3B (in the presence of CO) are compared with those of Fig. 4 (in the absence of CO). In both cases the catalyst temperature was set

TABLE 2  
Product Distributions for Methane Oxidation Under Reducing Conditions<sup>a</sup>

Catalysts	CH <sub>4</sub> Consumed (ppm)	CO <sub>2</sub> Produced (ppm)	CO Produced (ppm)	H <sub>2</sub> Produced (ppm)
Pt/Al <sub>2</sub> O <sub>3</sub>	1005	820	163	600
Pd/Al <sub>2</sub> O <sub>3</sub>	1000	800	250	715
Rh/Al <sub>2</sub> O <sub>3</sub>	1560	1025	560	2700

<sup>a</sup> 0.2 vol% CH<sub>4</sub> and 0.15 vol% O<sub>2</sub> in the feed, catalyst temperature = ~520°C, space velocity = 52 000 h<sup>-1</sup>.

at ~550°C and the feedstream concentration of CH<sub>4</sub> was held constant at 0.2 vol%. It is evident that an increase in the inlet O<sub>2</sub> concentration affects the CH<sub>4</sub> conversion in identical fashion regardless of whether or not CO is present in the feed. The only significant difference between Figs. 3B and 4 is that for each of the noble metals, a precipitous drop in CH<sub>4</sub> conversion occurs at a lower O<sub>2</sub> concentration in the absence of CO than it does in the presence of CO in the feed. Such a shift of the methane conversion curves toward lower O<sub>2</sub> concentrations in the CO-free feed of Fig. 4 is related to the fact that the stoichiometric amount of O<sub>2</sub> decreases from 0.45 to 0.40 vol% as 0.1 vol% CO is removed from the reactant stream.

For all three noble metal catalysts, methane oxidation under reducing conditions produced CO and H<sub>2</sub> as the principal products of partial oxidation. Our observation of H<sub>2</sub> as a reaction product during methane oxidation is perhaps not surprising in view of the report of Frennet (20) that at elevated temperatures methane chemisorption on noble metals is accompanied by H<sub>2</sub> evolution. Experiments conducted with feedstreams containing no CO were particularly convenient in examining the product distributions and the tendencies of the various noble metal catalysts to form CO during methane oxidation. Table 2 shows the amounts of CO, CO<sub>2</sub>, and H<sub>2</sub> produced and the amount of CH<sub>4</sub> consumed during methane oxidation under reducing conditions (0.2 vol% CH<sub>4</sub>, 0.15 vol% O<sub>2</sub>, and no CO in the feed) over the three noble metal catalysts at a catalyst

temperature of ~520°C. For each of the noble metal catalysts, there is a good correlation between the amount of CH<sub>4</sub> reacted and the sum of the amounts of CO and CO<sub>2</sub> produced during the methane oxidation (carbon balance closure to within 5%), indicating that CO and CO<sub>2</sub> are the only carbon-containing reaction products under our experimental conditions. (The presence of elemental carbon on the surface is ruled out because O<sub>2</sub> exposure of the catalyst following steady-state reaction at low O<sub>2</sub>/CH<sub>4</sub> ratios did not produce significant amounts of CO or CO<sub>2</sub>.) For all the runs conducted under reducing conditions, including those presented in Table 2, the mass balance for oxygen agreed within 10% when CO, CO<sub>2</sub>, H<sub>2</sub>, and H<sub>2</sub>O were assumed to be the only reaction products. Considering the uncertainty associated with the H<sub>2</sub> analysis (typical precision = ±5% of the reported value; our GC column was not optimized for H<sub>2</sub> analysis), it appears that no partial oxidation products other than CO and H<sub>2</sub> are formed in significant quantities under our reaction conditions. Although trace amounts of methanol, formaldehyde, and formic acid have also been reported as the reaction products in some cases (21), we did not pursue this point in detail.

The product selectivity to CO (i.e., the amount of CO produced divided by the amount of CH<sub>4</sub> consumed) for each noble metal can be calculated from the data of Table 2: 0.16 for Pt/Al<sub>2</sub>O<sub>3</sub>, 0.25 for Pd/Al<sub>2</sub>O<sub>3</sub>, and 0.36 for Rh/Al<sub>2</sub>O<sub>3</sub>. These calculated selectivities indicate that the ten-

dency to form the partial oxidation product CO decreases in the order  $\text{Rh}/\text{Al}_2\text{O}_3 > \text{Pd}/\text{Al}_2\text{O}_3 > \text{Pt}/\text{Al}_2\text{O}_3$ , in agreement with the ranking of the noble metal catalysts for CO conversion observed under the reducing feedstream conditions of Fig. 3. It is interesting to note that the  $\text{H}_2/\text{CO}$  ratio differs significantly among the noble metals:  $\sim 4$  for  $\text{Pt}/\text{Al}_2\text{O}_3$ ,  $\sim 3$  for  $\text{Pd}/\text{Al}_2\text{O}_3$ , and  $\sim 5$  for  $\text{Rh}/\text{Al}_2\text{O}_3$ . These compare with a  $\text{H}_2/\text{CO}$  ratio of 2 expected for the dissociative adsorption of methane leading to the cleavage of the C-H bond, a key step in methane oxidation over noble metals (7, 10, 11). This implies that for all three noble metals, the CO generated during the methane oxidation reacts more readily with oxygen than the  $\text{H}_2$ . In fact, the high  $\text{H}_2/\text{CO}$  ratio observed for the  $\text{Rh}/\text{Al}_2\text{O}_3$  catalyst is consistent with the results of separate reactor experiments with  $\text{CO}-\text{H}_2-\text{O}_2$  mixtures (22), which show that  $\text{Rh}/\text{Al}_2\text{O}_3$  is particularly effective in preferentially oxidizing CO in the presence of a large excess of  $\text{H}_2$ .

#### Oxidation Activity of Ceria-Promoted Noble Metal Catalysts in $\text{CH}_4-\text{CO}-\text{O}_2$ Mixtures

Since cerium is the most common base metal additive for commercial three-way catalyst formulations, it is of practical interest to examine how the activity and selectivity of the noble metal catalysts for methane oxidation are affected by the presence of Ce. Figure 5 shows the steady-state conversions of  $\text{CH}_4$  and CO over the  $\text{Pt}/\text{Ce}/\text{Al}_2\text{O}_3$ ,  $\text{Pd}/\text{Ce}/\text{Al}_2\text{O}_3$ , and  $\text{Rh}/\text{Ce}/\text{Al}_2\text{O}_3$  catalysts as a function of temperature in an oxidizing feedstream containing 0.2 vol%  $\text{CH}_4$ , 0.1 vol% CO, and 1 vol%  $\text{O}_2$ . It can be seen that the CO conversion characteristics under oxidizing conditions are similar with and without Ce; that is, as observed in Fig. 1A with the Ce-free noble metal catalysts, the CO in the feed was completely reacted over  $\text{Pt}/\text{Ce}/\text{Al}_2\text{O}_3$  and  $\text{Pd}/\text{Ce}/\text{Al}_2\text{O}_3$  at temperatures as low as  $\sim 220^\circ\text{C}$  while a substantially higher temperature ( $\sim 320^\circ\text{C}$ ) was required

for complete CO conversion over  $\text{Rh}/\text{Ce}/\text{Al}_2\text{O}_3$ . In contrast, comparison of Figs. 1B and 5B shows that the  $\text{CH}_4$  oxidation activity of  $\text{Pt}/\text{Al}_2\text{O}_3$  and  $\text{Pd}/\text{Al}_2\text{O}_3$  under oxidizing conditions is retarded markedly in the presence of Ce. The activity of the  $\text{Rh}/\text{Al}_2\text{O}_3$  catalysts for  $\text{CH}_4$  oxidation was observed to be little affected by Ce, however. The Ce-induced suppression of the  $\text{CH}_4$  oxidation activity was observed to be most dramatic for  $\text{Pd}/\text{Al}_2\text{O}_3$  ( $\sim 200^\circ\text{C}$  increase in the 50% conversion temperature); consequently, the activity ranking in the presence of excess  $\text{O}_2$  changes from  $\text{Pd} > \text{Rh} > \text{Pt}$  without Ce (Fig. 1B) to  $\text{Rh} > \text{Pd} \approx \text{Pt}$  with Ce (Fig. 5B). A similar detrimental effect of Ce addition was reported for the oxidation of other saturated hydrocarbons (such as  $n\text{-C}_4\text{H}_{10}$ ) over  $\text{Pt}/\text{Al}_2\text{O}_3$  and  $\text{Pd}/\text{Al}_2\text{O}_3$  (10). Under the strongly oxidizing conditions of Fig. 5, all the Ce-containing noble metal catalysts promoted the complete oxidation of  $\text{CH}_4$  to  $\text{CO}_2$  and  $\text{H}_2\text{O}$ .

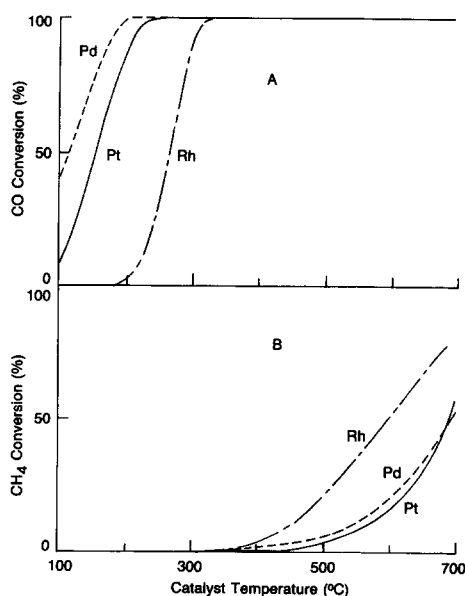


FIG. 5. Conversions of CO (A) and  $\text{CH}_4$  (B) over the ceria-promoted alumina-supported noble metal catalysts as a function of temperature in an oxidizing feedstream containing 0.2 vol%  $\text{CH}_4$ , 0.1 vol% CO, and 1 vol%  $\text{O}_2$ .



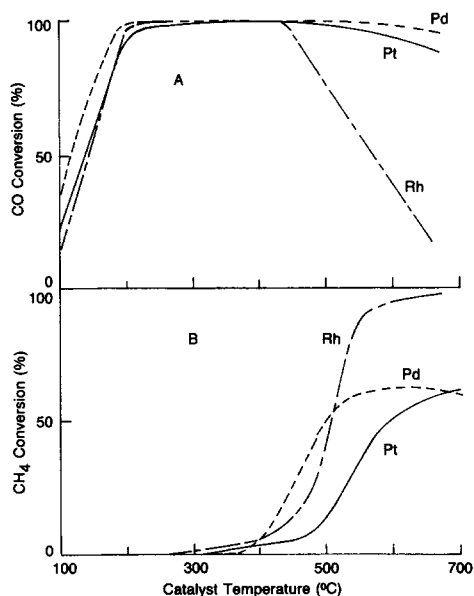


FIG. 6. Conversions of CO (A) and CH<sub>4</sub> (B) over the ceria-promoted alumina-supported noble metal catalysts as a function of temperature in a reducing feedstream containing 0.2 vol% CH<sub>4</sub>, 0.1 vol% CO, and 0.33 vol% O<sub>2</sub>.

Shown in Fig. 6 are the results of temperature run-up experiments with the Ce-containing noble metal catalysts in a reducing feedstream containing 0.2 vol% CH<sub>4</sub>, 0.1 vol% CO, and 0.33 vol% O<sub>2</sub>. All three Ce-containing noble metal catalysts exhibit similar low-temperature CO oxidation activity, achieving nearly complete CO conversion at ~220°C. The CO conversion over Pt/Ce/Al<sub>2</sub>O<sub>3</sub> and Pd/Ce/Al<sub>2</sub>O<sub>3</sub> remained high (>90%) as the temperature was increased up to 650°C. Over the Rh/Ce/Al<sub>2</sub>O<sub>3</sub> catalyst, on the other hand, complete CO conversion was maintained only up to ~450°C; the CO conversion declined gradually with a further increase in temperature (to a 20% level at 650°C). Comparison of Figs. 2B and 6B reveals that for each of the noble metals, the temperature required for the onset of the CH<sub>4</sub> reaction in the reducing feedstream is little affected by the presence of cerium in the catalysts. Note, however, that the CH<sub>4</sub> conversion levels reached at elevated tem-

peratures over Pt/Ce/Al<sub>2</sub>O<sub>3</sub> and Pd/Ce/Al<sub>2</sub>O<sub>3</sub> (~65%) are substantially lower than those over the Ce-free counterparts (85–90%). The lower CH<sub>4</sub> conversion levels observed at high temperatures for the Ce-containing Pt/Al<sub>2</sub>O<sub>3</sub> and Pd/Al<sub>2</sub>O<sub>3</sub> catalysts appear to be a direct consequence of their tendency to promote the total oxidation of CH<sub>4</sub>. In this high-temperature, oxygen-deficient regime, the CH<sub>4</sub> conversion would likely be limited by the oxygen availability and thus a lower CH<sub>4</sub> conversion is expected for the total oxidation of CH<sub>4</sub> than for the partial oxidation. In fact, assuming 100% conversion of the CO in the feed and the total oxidation of methane, the highest possible CH<sub>4</sub> conversion at the 0.33 vol% inlet O<sub>2</sub> level is calculated to be 70%, in close agreement with the maximum conversion of ~65% observed in Fig. 6B for Pt/Ce/Al<sub>2</sub>O<sub>3</sub> and Pd/Ce/Al<sub>2</sub>O<sub>3</sub>. In contrast, the presence of Ce in the Rh/Al<sub>2</sub>O<sub>3</sub> catalyst did not significantly alter the CH<sub>4</sub> conversion at high temperatures; just as we saw with the Ce-free Rh/Al<sub>2</sub>O<sub>3</sub> catalyst (Fig. 2B), the CH<sub>4</sub> conversion over Rh/Ce/Al<sub>2</sub>O<sub>3</sub> approached 100% in the high-temperature regime, but only at the expense of decreased CO conversion. Thus, under the reducing conditions of Fig. 6, the activity and product selectivity of Rh/Al<sub>2</sub>O<sub>3</sub> for CH<sub>4</sub> oxidation are virtually unaffected by the presence of Ce, whereas the addition of Ce to Pt/Al<sub>2</sub>O<sub>3</sub> and Pd/Al<sub>2</sub>O<sub>3</sub> suppresses the formation of the partial oxidation product CO (with the concomitant decrease in CH<sub>4</sub> conversion at elevated temperatures).

Another aspect of cerium's contribution to the performance of the noble metal catalysts during methane oxidation at ~550°C is depicted in Fig. 7. Recall that over the Ce-free noble metal catalysts (Fig. 3B), the CH<sub>4</sub> conversion goes through a maximum as the inlet O<sub>2</sub> concentration is increased before the conversion drops precipitously near the stoichiometric O<sub>2</sub> concentration of 0.45 vol%. The Ce-containing Pd/Al<sub>2</sub>O<sub>3</sub> and Rh/Al<sub>2</sub>O<sub>3</sub> catalysts (Fig. 7B) show the same behavior; that is, the CH<sub>4</sub> conversion declines

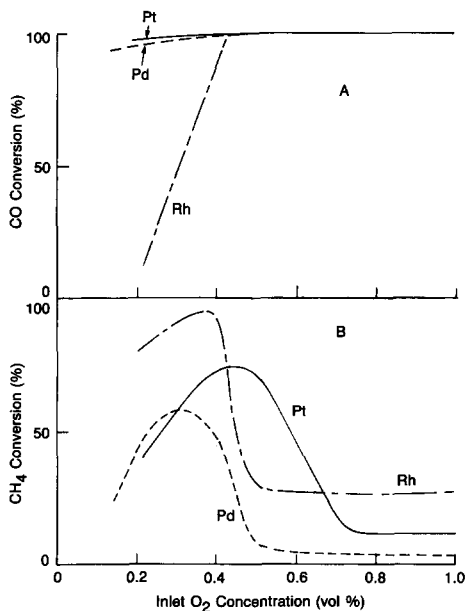


FIG. 7. Conversions of CO (A) and  $\text{CH}_4$  (B) over the ceria-promoted alumina-supported noble metal catalysts at a catalyst temperature of  $550^\circ\text{C}$  in feedstreams containing 0.2 vol%  $\text{CH}_4$ , 0.1 vol% CO, and variable levels of  $\text{O}_2$ .

sharply when a near-stoichiometric amount of  $\text{O}_2$  (0.4 to 0.5 vol%) is present in the feed. It is important to note, however, that the Pt/Ce/ $\text{Al}_2\text{O}_3$  catalyst stands alone in its ability to maintain relatively high  $\text{CH}_4$  conversions in a feedstream that contains a considerable excess of  $\text{O}_2$ . This suggests the possibility of widening the air/fuel ratio "window" in the operation of actual natural-gas vehicles by adding Ce to Pt/ $\text{Al}_2\text{O}_3$  catalysts.

Figure 7A shows the CO conversion data over the Ce-containing noble metal catalysts obtained during the same variable  $\text{O}_2$  concentration experiments discussed above. In accordance with the temperature run-up data of Fig. 6A, the CO conversion over Pt/Ce/ $\text{Al}_2\text{O}_3$  and Pd/Ce/ $\text{Al}_2\text{O}_3$  remains high (>95%) throughout the entire  $\text{O}_2$  concentration range considered here. This points to the tendency of the Ce-containing Pt/ $\text{Al}_2\text{O}_3$  and Pd/ $\text{Al}_2\text{O}_3$  catalysts to oxidize  $\text{CH}_4$  to  $\text{CO}_2$  (rather than CO) even under extremely oxygen-deficient conditions. Separate ex-

periments with the same Pt/Ce/ $\text{Al}_2\text{O}_3$  and Pd/Ce/ $\text{Al}_2\text{O}_3$  catalysts but with feeds containing only  $\text{CH}_4$  and  $\text{O}_2$  confirmed that the amount of CO produced as a result of partial oxidation of methane was indeed minimal. Unlike the cases with Pt/Ce/ $\text{Al}_2\text{O}_3$  and Pd/Ce/ $\text{Al}_2\text{O}_3$ , a substantial amount of CO was produced over the Rh/Ce/ $\text{Al}_2\text{O}_3$  catalyst under the reducing conditions of Fig. 7, where a limited amount of  $\text{O}_2$  reacted with a mixture of  $\text{CH}_4$  and CO. Rhodium exhibits such a tendency to form CO during methane oxidation regardless of whether or not Ce is present in the catalyst, as evidenced by the close similarity between the CO conversion curves in Figs. 3A and 7A.

Figures 6 and 7 reveal that the high CO conversions achieved over the Pt/Ce/ $\text{Al}_2\text{O}_3$  and Pd/Ce/ $\text{Al}_2\text{O}_3$  catalysts under reducing conditions are accompanied by the relatively low  $\text{CH}_4$  conversions (compared to those for their Ce-free counterparts shown in Figs. 2 and 3). This indicates that as Ce is added to Pt/ $\text{Al}_2\text{O}_3$  and Pd/ $\text{Al}_2\text{O}_3$ , the increased CO conversion under reducing conditions is offset to some degree by the loss in  $\text{CH}_4$  conversion efficiency. The appropriate trade-offs for practical emission control are beyond the scope of this laboratory study.

## DISCUSSION

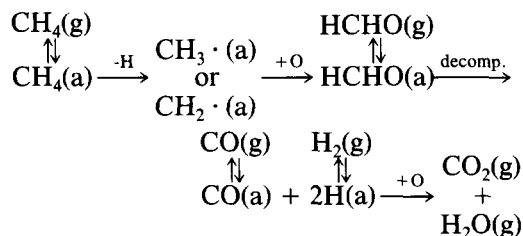
### *Reaction Mechanism for Methane Oxidation*

Under the oxidizing feedstream conditions considered here, the noble metal surface is predominantly covered with oxygen and thus the critical step in the methane oxidation is the dissociative adsorption (and subsequent reaction) of  $\text{CH}_4$  onto the oxygen-covered surface (10, 11, 23-25). The supporting evidence for this conclusion is given below. First, most kinetic studies conducted over noble metal catalysts in the presence of excess  $\text{O}_2$  show that the observed rate law is first order in methane and zero order in oxygen (11, 19, 24). Second, oxygen adsorption on noble metals is fast under the reaction conditions considered here (26), whereas methane adsorption is a

slow, activated process (20). As a result of the substantial difference in adsorption strengths ( $O_2 > CH_4$ ),  $O_2$  inhibits the  $CH_4$  oxidation under oxidizing conditions by excluding the more weakly adsorbed species,  $CH_4$ , from the active sites, as observed in Figs. 3B, 4, and 7B. (The presence of CO in the feed would probably not significantly change the relative surface concentration of  $CH_4$  and  $O_2$  under reaction conditions, because CO tends to desorb rapidly from the surface at the high temperatures required for the methane reaction.) As the  $O_2$  concentration in the feed is decreased to less than the stoichiometric value (while holding the concentration of the reducing agents constant), however,  $CH_4$  can compete successfully with  $O_2$  for the active sites despite its weaker adsorption strength. In this case, the adsorption rates for both reactants would become comparable, yielding a high reaction rate and thus high  $CH_4$  conversion. With a further decrease in inlet  $O_2$  concentration, insufficient amounts of  $O_2$  adsorb on the surface and the  $CH_4$  conversion becomes low because of the resulting kinetic and/or stoichiometric limitations encountered during the methane oxidation. This explains why the  $CH_4$  conversion goes through a maximum as the inlet  $O_2$  concentration is varied, as illustrated in Figs. 3B, 4, and 7B. A similar dependence of methane conversion on exhaust stoichiometry, including a maximum  $CH_4$  conversion under somewhat richer than stoichiometric conditions, was observed over commercial noble metal catalysts in a recent engine-dynamometer study with methane fuel (27).

The detailed mechanism of methane oxidation on noble metals is not yet well understood. Methane chemisorption and methane-deuterium exchange experiments (20, 28) have shown that the chemisorption of methane on noble metals involves dissociation to adsorbed methyl or methylene radicals, as a result of removal of hydrogen atoms from the carbon atom. The subsequent interaction of methyl or methylene radicals with adsorbed oxygen has been pro-

posed to lead to either direct oxidation to  $CO_2$  and  $H_2O$  or the formation of chemisorbed formaldehyde via methoxide, methyl peroxide, or methylene oxide intermediates (7, 23, 29, 30). Recent studies of formaldehyde oxidation on Pt by McCabe and McCready (31) and by Lapinski *et al.* (32) provided kinetic and spectroscopic evidence that the oxidation reaction involves the dissociation of the adsorbed formaldehyde to adsorbed CO and adsorbed H atoms. These adsorbed CO and H atoms have been observed to either desorb as CO and  $H_2$  or react with adsorbed oxygen to produce  $CO_2$  and  $H_2O$ , depending on the stoichiometry of the reactant gas mixture (31, 32). Based on the above discussion, the proposed reaction mechanism for methane oxidation can be summarized as



The mechanism proposed above is consistent with our observation of CO,  $CO_2$ ,  $H_2$ , and  $H_2O$  as the principal reaction products of the methane oxidation under reducing conditions. Although not directly measured, material balance considerations indicate that no significant amount of gaseous formaldehyde was produced during the methane oxidation over the noble metal catalysts. This suggests that under our reaction conditions an adsorbed formaldehyde intermediate, once formed, may rapidly decompose to  $CO(a)$  and  $H(a)$  rather than desorb into the gas phase as formaldehyde molecules.

Given the presence of CO,  $CO_2$ ,  $H_2$ , and  $H_2O$  in the reaction mixture, it is possible that the product distribution for the methane oxidation may be altered by the water-gas shift equilibrium reaction

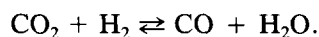


TABLE 3  
Methane Conversion and CO Production With and Without CO<sub>2</sub> Addition

	Pt/Al <sub>2</sub> O <sub>3</sub>		Pd/Al <sub>2</sub> O <sub>3</sub>		Rh/Al <sub>2</sub> O <sub>3</sub>	
	CH <sub>4</sub> Conv. (%)	CO (ppm)	CH <sub>4</sub> Conv. (%)	CO (ppm)	CH <sub>4</sub> Conv. (%)	CO (ppm)
Base case <sup>a</sup>	50	163	50	250	78	560
1000 ppm CO <sub>2</sub> Added	51	177	52	275	76	687
2000 ppm CO <sub>2</sub> Added	51	181	50	250	76	750

<sup>a</sup> 0.2 vol% CH<sub>4</sub> and 0.15 vol% O<sub>2</sub> in the feed (no CO<sub>2</sub> added), catalyst temperature = ~520°C, space velocity = 52 000 h<sup>-1</sup>.

The equilibrium constant for the reaction as written above is sufficiently large under our experimental conditions (0.25 at 525°C) so that a significant amount of CO can be formed from the CO<sub>2</sub> and H<sub>2</sub> produced during the methane oxidation. In fact, such a reaction mechanism has recently been proposed by Ashcroft *et al.* (33) for selective oxidation of methane to synthesis gas over transition metal catalysts. The importance of the water-gas shift equilibrium to the activity and product selectivity for our methane oxidation experiments was examined by first establishing a steady-state reaction condition at ~520°C with a reducing feedstream containing 0.2 vol% CH<sub>4</sub> and 0.15 vol% O<sub>2</sub> and then adding CO<sub>2</sub> stepwise to the feedstream while holding the temperature and total flow rate constant. This experimental verification is based on the fact that if the shift reaction is operative in our system, the addition of CO<sub>2</sub> to the feed should increase CO production. (Adding CO<sub>2</sub>, rather than H<sub>2</sub>, is preferable because it allows one to probe the shift reaction without perturbing the feedstream stoichiometry.) The results of such experiments for the three alumina-supported noble metal catalysts are presented in Table 3, which lists methane conversions and the amounts of CO produced during methane oxidation with and without CO<sub>2</sub> addition to the feed. (A more detailed description of the product distribution for the base case is given in Table 2.) It can be seen that for each of the noble metal

catalysts the methane conversion is independent of the CO<sub>2</sub> level in the reaction mixture. The amount of CO produced over either Pt/Al<sub>2</sub>O<sub>3</sub> or Pd/Al<sub>2</sub>O<sub>3</sub> is also virtually unaffected by the CO<sub>2</sub> addition. For the Rh/Al<sub>2</sub>O<sub>3</sub> catalyst, on the other hand, increasing the CO<sub>2</sub> level in the reaction mixture tends to enhance CO production (and, although not shown, suppress H<sub>2</sub> production) during the methane oxidation. This suggests that the water-gas shift reaction plays a significant role in determining the product selectivity for methane oxidation over Rh/Al<sub>2</sub>O<sub>3</sub>, but not over Pt/Al<sub>2</sub>O<sub>3</sub> or Pd/Al<sub>2</sub>O<sub>3</sub>. The insensitivity of the methane conversions over the noble metals to the CO<sub>2</sub> level in the feed suggests that the rate-limiting step in the methane oxidation, which is generally believed to be the dissociation of adsorbed methane molecules (10, 11), is unaffected by CO<sub>2</sub>.

#### *Effects of Ce Additive on Catalytic Properties*

Comparison of Figs. 1B and 5B shows that the methane oxidation activity of Rh/Al<sub>2</sub>O<sub>3</sub> under oxidizing conditions is not significantly affected by the presence of Ce. In contrast, the methane conversions over the Pt/Ce/Al<sub>2</sub>O<sub>3</sub> and Pd/Ce/Al<sub>2</sub>O<sub>3</sub> catalysts were observed to be considerably lower than those over the Ce-free counterparts. The detrimental effect of Ce addition on the methane oxidation activity is particularly pronounced for Pd; the 50% conversion

temperature increased by nearly 200°C when Ce was added to the Pd/Al<sub>2</sub>O<sub>3</sub> catalyst. A similar activity suppression by Ce was also observed for the oxidation of other alkanes (C<sub>3</sub>H<sub>8</sub> and C<sub>4</sub>H<sub>10</sub>) over Pd/Al<sub>2</sub>O<sub>3</sub> in the presence of excess oxygen (10, 34). The low alkane oxidation activities observed over Ce-containing Pd/Al<sub>2</sub>O<sub>3</sub> catalysts under oxidizing conditions have been shown to be related to the tendency of the Ce to promote the formation of bulk oxide of palladium (34), which is much less active for methane oxidation than the surface oxygen on the palladium crystallites (24, 35). A similar metal–ceria interaction has been reported for the Pt/Ce/Al<sub>2</sub>O<sub>3</sub> system; Summers and Ausen (36) and Yu Yao (10) presented IR and kinetic evidence to suggest that Ce promotes/stabilizes an oxidized platinum species. Thus, the Ce-induced suppression of the methane oxidation activity over Pt/Al<sub>2</sub>O<sub>3</sub> (~70°C increase in the 50% conversion temperature) can be attributed to the Pt being converted into a less active, oxidized state as a result of interaction with the Ce. Ce may interact with Rh in the same way as with Pt or Pd; however, since the oxidation state of the Rh/Al<sub>2</sub>O<sub>3</sub> surface changes readily in response to a change in its gaseous environment at temperatures above 200°C (12, 37), the extent and stability of Rh oxide formation under our reaction conditions are likely to be dominated by the stoichiometry of the reactant gas mixture rather than by the presence of Ce. This may explain why the Rh/Al<sub>2</sub>O<sub>3</sub> catalyst with and without Ce exhibits similar methane oxidation activity in the oxidizing feedstream of Figs. 1 and 5.

The observation that the kinetic behavior of Rh/Al<sub>2</sub>O<sub>3</sub> is not affected by Ce carries over to the reducing feedstream conditions employed in Figs. 2 and 6, where the conversions of both CH<sub>4</sub> and CO over Rh/Al<sub>2</sub>O<sub>3</sub> were observed to be similar to those over Rh/Ce/Al<sub>2</sub>O<sub>3</sub>. Particularly noteworthy in Fig. 6 is the observation that unlike their Ce-free counterparts, the Pt/Ce/Al<sub>2</sub>O<sub>3</sub> and Pd/Ce/Al<sub>2</sub>O<sub>3</sub> catalysts maintain high (>90%) CO conversions even at high temperatures

(>450°C) where the methane oxidation becomes significant. This indicates the tendencies of Ce-containing Pt/Al<sub>2</sub>O<sub>3</sub> and Pd/Al<sub>2</sub>O<sub>3</sub> to produce only minimal amounts of CO during methane oxidation under reducing conditions. The underlying reasons for the suppression of CO formation over Pt/Ce/Al<sub>2</sub>O<sub>3</sub> and Pd/Ce/Al<sub>2</sub>O<sub>3</sub> are uncertain. One possible explanation might be that in the presence of Ce, adsorbed CO on the noble metals (generated from partial oxidation of methane) reacts readily with surface oxygen derived from the neighboring ceria particles to produce CO<sub>2</sub> before it desorbs as gaseous CO. In this case, the limited supply of O<sub>2</sub> in the feed would be consumed by the partial oxidation product CO in preference to the CH<sub>4</sub> over the ceria-promoted Pt and Pd catalysts, resulting in relatively low levels of CH<sub>4</sub> conversion under reducing conditions as illustrated in Figs. 6 and 7. In fact, the methane conversion efficiencies observed in Fig. 6B for the Ce-containing Pt and Pd catalysts at high temperatures are close to a maximum methane conversion (70%) expected when assuming that none of the CH<sub>4</sub> in the feed is partially oxidized to CO in the presence of Ce. In contrast to Pt/Al<sub>2</sub>O<sub>3</sub> and Pd/Al<sub>2</sub>O<sub>3</sub>, the CO conversion characteristics of Rh/Al<sub>2</sub>O<sub>3</sub> are virtually unaffected by Ce (compare Figs. 2A and 6A). This implies that the nature of metal–ceria interaction in Rh/Ce/Al<sub>2</sub>O<sub>3</sub> might be different from that in Pt/Ce/Al<sub>2</sub>O<sub>3</sub> or Pd/Ce/Al<sub>2</sub>O<sub>3</sub>. Also, this difference in CO conversion characteristics among the Ce-containing noble metal catalysts may be related to the fact that the water–gas shift reaction plays a significant role in determining the product selectivity of Rh/Al<sub>2</sub>O<sub>3</sub>, but not Pt/Al<sub>2</sub>O<sub>3</sub> or Pd/Al<sub>2</sub>O<sub>3</sub>. Further work is required to clarify the role of Ce in modifying the kinetics of methane oxidation over noble metals.

#### *Hysteresis in Methane Oxidation Activity over Pd/Al<sub>2</sub>O<sub>3</sub>*

All the temperature run-up data reported here represent stabilized activities and selectivities measured by carrying out repetitive runs in the feedstream of interest with

the catalyst samples initially calcined in air for 4 h at 500°C. The results of the variable O<sub>2</sub> concentration experiments shown in Figs. 3, 4, and 7 were generated by first heating the sample to the desired temperature (~550°C) in a strongly reducing feedstream and then adding O<sub>2</sub> stepwise to the feed, with the temperature, total flow rate, and CH<sub>4</sub> and CO concentrations held constant. In order to investigate how the catalytic behavior is affected by the sample history, we conducted additional variable O<sub>2</sub> concentration experiments at ~550°C with the Ce-free noble metal catalysts by decreasing the O<sub>2</sub> concentration in the feed step-by-step starting from an oxidized state of the catalyst. For Pt/Al<sub>2</sub>O<sub>3</sub> and Rh/Al<sub>2</sub>O<sub>3</sub>, the results of such experiments were found to be similar to those of the original variable O<sub>2</sub> concentration experiments shown in Figs. 3 and 4, indicating that these two catalysts arrived at essentially the same final steady-state condition regardless of whether they started from a reduced or an oxidized state. However, the oxidation activity of the Pd/Al<sub>2</sub>O<sub>3</sub> catalyst is a strong function of its prior history; that is, plots of methane conversion vs O<sub>2</sub> concentration at a catalyst inlet temperature of ~550°C followed drastically different paths depending on the direction of O<sub>2</sub> concentration change, as depicted in Fig. 8 for feedstreams containing 0.2 vol% CH<sub>4</sub>, 0.1 vol% CO, and variable levels of O<sub>2</sub>. (The CO conversion over Pd/Al<sub>2</sub>O<sub>3</sub>, on the other hand, was not significantly different.) A transition from the low conversion branch to the high conversion branch in the net-oxidizing regime of Fig. 8 could not be achieved simply by varying the O<sub>2</sub> concentration in the feed. It was found, however, that cooling the reactor to ≤300°C in He followed by a run-up to ~550°C in a strongly oxidizing reactant mixture (e.g., one containing 1 vol% O<sub>2</sub>) was effective in restoring the high activity state of the Pd/Al<sub>2</sub>O<sub>3</sub> catalyst. This points to the importance of a low-temperature exposure to an oxidizing environment in reactivating the Pd/Al<sub>2</sub>O<sub>3</sub> catalyst. Although the detailed

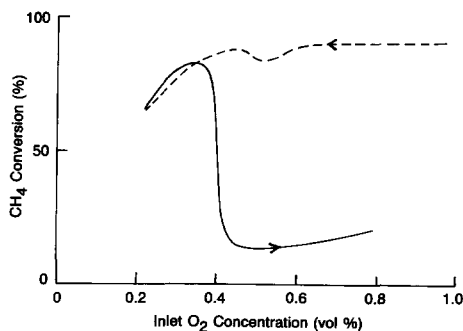


FIG. 8. Effects of the direction of O<sub>2</sub> concentration change on methane conversion over Pd/Al<sub>2</sub>O<sub>3</sub> at a catalyst temperature of 550°C in feedstreams containing 0.2 vol% CH<sub>4</sub>, 0.1 vol% CO, and variable levels of O<sub>2</sub>.

mechanism for the catalyst activation process is not certain at this time, it is likely that the activity enhancement arises from the high reactivity of surface oxygen covering the Pd crystallites, which has been reported to form in an oxidizing environment at low temperatures (24, 38, 39). During a high-temperature oxidizing treatment of palladium, on the other hand, the surface oxygen species has been shown to migrate into the bulk, forming unreactive Pd bulk oxide (24, 38, 39). This would explain the low methane oxidation activity observed at high O<sub>2</sub> concentrations on the lower branch of Fig. 8. Also, once activated by a low-temperature oxidizing treatment, the oxygen coverage on the Pd surface during methane oxidation may be well below the saturation limit as a result of depletion of surface oxygen by the reaction. Since oxygen penetration into the bulk is generally believed to occur from an oxygen-saturated surface (38), it is possible that, once activated in a low-temperature oxidizing environment, the Pd/Al<sub>2</sub>O<sub>3</sub> catalyst remains resistant to bulk oxide formation (and thus retains its high activity state, as observed) during the subsequent run-up to 550°C in an oxidizing feedstream. Further work is required to better understand the structure-activity relationship for Pd in general, and to verify the above-mentioned catalyst reactivation mechanism in particular.

## REFERENCES

1. Weaver, C. S., SAE Paper No. 892133.
2. Martin, W. F., and Campbell, S. L., "Natural Gas: A Strategic Resource for the Future." Washington Policy and Analysis, Washington, DC, 1988.
3. Golomb, D., and Fay, J. A., "The Role of Methane in Tropospheric Chemistry." Energy Laboratory, Cambridge, MA, 1989.
4. DeLuchi, M. A., Johnston, R. A., and Sperling, D., SAE Paper No. 881656.
5. Hillemann, B., *Chem. Eng. News* **67**(11), 25 (1989).
6. Cadle, S. H., Mulawa, P. A., Hilden, D. L., and Halsall, R., "Exhaust Emissions from Dual-Fuel Vehicles Using Compressed Natural Gas and Gasoline," presented to the Air and Water Management Association, Pittsburgh, PA, 1990.
7. Golodets, G. I., "Heterogeneous Catalytic Reactions Involving Molecular Oxygen," Studies in Surface Science and Catalysis, Vol. 15, Chap. 15. Elsevier, Amsterdam, 1983.
8. Anderson, R. B., Stein, K. C., Feenan, J. J., and Hofer, L. J. E., *Ind. Eng. Chem.* **53**, 809 (1961).
9. Firth, J. G., and Holland, H. B., *Faraday Soc. Trans.* **65**, 1121 (1969).
10. Yu Yao, Y.-F., *Ind. Eng. Chem. Prod. Res. Dev.* **19**, 293 (1980).
11. Otto, K., *Langmuir* **5**, 1364 (1989).
12. Schlatter, J. C., Taylor, K. C., and Sinkevitch, R. M., "The Behavior of Supported Rhodium in Catalyzing CO and NO Reactions," presented at Adv. in Catal. Chem. Symp., Snowbird, UT, 1979.
13. Dictor, R., and Roberts, S., *J. Phys. Chem.* **93**, 2526 (1989).
14. Oh, S. H., and Eickel, C. C., *J. Catal.* **112**, 543 (1988).
15. McCabe, R. W., and Mitchell, P. J., *Ind. Eng. Chem. Prod. Res. Dev.* **23**, 196 (1984).
16. Voltz, S. E., Morgan, C. R., Liederman, D., and Jacob, S. M., *Ind. Eng. Chem. Prod. Res. Dev.* **12**, 294 (1973).
17. McCabe, R. W., and Mitchell, P. J., *Appl. Catal.* **27**, 83 (1986).
18. Kummer, J. T., *Prog. Energy Combust. Sci.* **6**, 177 (1980).
19. Niwa, M., Awano, K., and Murakami, Y., *Appl. Catal.* **7**, 317 (1983).
20. Frennet, A., *Catal. Rev.-Sci. Eng.* **10**, 37 (1974).
21. Margolis, L. Y., in "Advances in Catalysis" (D. D. Eley, H. Pines, and P. B. Weisz, Eds.), Vol. 14, p. 429. Academic Press, New York, 1963.
22. Sinkevitch, R. M., and Oh, S. H., "A Method and Apparatus for Selective Removal of Carbon Monoxide," U.S. Patent filed, SN #709,563, 1991.
23. Cullis, C. F., Keene, D. E., and Trimm, D. L., *J. Catal.* **19**, 378 (1970).
24. Cullis, C. F., and Willatt, B. M., *J. Catal.* **83**, 267 (1983).
25. Hicks, R. F., Qi, H., Young, M. L., and Lee, R. G., *J. Catal.* **122**, 280 (1990).
26. Engel, T., and Ertl, G., in "Advances in Catalysis" (D. D. Eley, H. Pines, and P. B. Weisz, Eds.), Vol. 28, p. 1. Academic Press, New York, 1979.
27. Siewert, R. M., and Mitchell, P. J., General Motors Research Laboratories, Warren, MI, unpublished results, 1990.
28. Kemball, C., in "Advances in Catalysis" (D. D. Eley, P. W. Selwood, and P. B. Weisz, Eds.), Vol. 11, p. 223, Academic Press, New York, 1959.
29. Dowden, D. A., Schnell, C. R., and Walker, G. T., in "Proceedings, 4th International Congress on Catalysis, Moscow, 1968" (B. A. Kazansky, Ed.), p. 1120. Adler, New York, 1968.
30. Pitchai, R., and Klier, K., *Catal. Rev.-Sci. Eng.* **28**, 13 (1986).
31. McCabe, R. W., and McCready, D. F., *Chem. Phys. Lett.* **111**, 89 (1984).
32. Lapinski M. P., Silver, R. G., Ekerdt, J. G., and McCabe, R. W., *J. Catal.* **105**, 258 (1987).
33. Ashcroft, A. T., Cheetham, A. K., Foord, J. S., Green, M. L. H., Grey, C. P., Murrell, A. J., and Vernon, P. D. F., *Nature* **344**, 319 (1990).
34. Shyu, J. Z., Otto, K., Watkins, W. L. H., Graham, G. W., Belitz, R. K., and Gandhi, H. S., *J. Catal.* **114**, 23 (1988).
35. Hicks, R. F., Qi, H., Young, M. L., and Lee, R. G., *J. Catal.* **122**, 295 (1990).
36. Summers, J. C., and Ausen, S. A., *J. Catal.* **58**, 131 (1979).
37. Oh, S. H., and Carpenter, J. E., *J. Catal.* **80**, 472 (1983).
38. Campbell, C. T., Foyt, D. C., and White, J. M., *J. Phys. Chem.* **81**, 491 (1977).
39. Conrad, H., Ertl, G., Kupperts, J., and Latta, E. E., *Surf. Sci.* **65**, 245 (1977).